
Article:
Vigor, J.E., Bernal, S.A., Xiao, X. et al. (1 more author) (2020) Automated correction for the movement of suspended particulate in microtomographic data. Chemical Engineering Science, 223. 115736. ISSN 0009-2509

https://doi.org/10.1016/j.ces.2020.115736

Automated correction for the movement of suspended particulate in microtomographic data

James E. Vigor[a,b], Susan A. Bernal[a,b], Xianghui Xiao[c,d], and John L. Provis[a]*

a. Department of Materials Science and Engineering, The University of Sheffield, Sheffield S1 3JD, United Kingdom

b. School of Civil Engineering, University of Leeds, Leeds LS2 9JT, United Kingdom

c. Argonne National Laboratory, 9700 S. Cass Avenue, Lemont, IL 60439, United States

d. Office 365, Brookhaven National Lab, PO Box 5000, Upton, NY 11973-5000, United States

* Corresponding author. Email j.provis@sheffield.ac.uk

Abstract

This study reports the development and application of a digital image cross correlation based approach to resolve contiguous microstructural volumes of interest in X-ray microtomography data, collected in fluid suspensions that undergo significant microstructural changes over time, using fresh cementitious pastes as an example. This computational method provides a high precision both for cementitious pastes that sediment only slightly (i.e. are cohesive), and for those that undergo significant sedimentation and/or settlement within the first few minutes of reaction. The normalised cross correlation algorithm presented here enables the observation of an identical volume of interest, i.e., one which contains a contiguous particle group, from the first seconds of observation onwards with excellent accuracy. This method enables segmentation of the same cluster of particles to be almost entirely automated and resolved in large sets of sequentially collected data, therefore enabling particle reaction to be observed directly while removing effects due to sedimentation.

Introduction

Computerised micro-tomography provides a three dimensional stack of images that non-destructively reveal sequential cross-sections through the depth of a sample. Using this method, both slowly evolving or static [1, 2] and dynamic processes [3] may be observed on a micron to sub-micron length scale, and potentially at a very high acquisition rate when using advanced modern instrumentation [4]. This technique has been extensively shown to allow both the observation and quantification of the microstructure, and microstructural evolution, of geological [5], cementitious [6-8] and biological [9, 10] specimens. However, it is difficult to accurately locate a particular particle, or group of particles, in hundreds of tomographic stacks describing the dynamically changing microstructure of a system that is fluid and reacting and/or sedimenting in-situ during an experiment. As the particulate component of a slurry or suspension settles within a capillary sample that is being tomographically analysed, material has a tendency to move significantly in all three coordinate axes as the sample rotates and particles are subjected to gravitational effects. It is therefore challenging to track a single region (particle or cluster) of interest across a large quantity of scans, particularly when a large number of particles are present within the sample volume. This raises a significant limitation in the ability to isolate and analyse the reaction of single particles which do not remain in a constant location within the overall sample.

The hydration reaction of Portland cement is an ideal case study for a reaction process involving simultaneous reaction and sedimentation in a particulate suspension. Upon mixing cement powder and water, a fluid suspension is formed, and the hydration of the silicate and aluminate phases present within the cement begins immediately. The cement particles are relatively unrestricted in their movement within the localised geometry of the fluid suspension until they react and a significant quantity of new hydrous cementitious binder phases form, solidifying the paste. This movement becomes problematic when it is desirable to follow and analyse the reaction of a given particle (requiring segmentation of a contiguous target volume) via in an in-situ experiment during the first hours of reaction. It is incredibly challenging to accurately isolate and follow a particular particle or unique volume throughout the

desired duration using the human eye. To reduce problems of sedimentation and segregation during analysis of fresh cement pastes, chemical additives may be used to modify the viscosity of the paste and reduce segregation of particles [11]. However, to prevent admixtures from modifying chemico-physical interactions [12] within the reacting cement paste, and thus to ensure that the reaction process of the model system remains representative, the addition of such organic compounds may be undesirable.

Additionally, when materials are analysed in-situ over a longer duration, or removed then re-inserted to and from the analysis position in an imaging instrument, movement of the specimen within the field of view of the instrument may also result in variations between successive data sets. It is inappropriate to assume that the target volume remains in the precisely the same location in all three axes over an extended testing timeframe.

In this paper, a novel correction method to account for time-variable geometric features in particulate suspensions undergoing rapid spatial movement (i.e. sedimentation of cement grains and release of entrapped air) is presented. We apply the method to aiding in the tomographic analysis of materials which show large changes, and also those which stabilise more rapidly, and demonstrate that the proposed methodology can handle these magnitudes of deviations from the original suspension geometry.

Digital Volume and Image Cross Correlation

Digital volume correlation has been commonly applied for strain measurement in microtomographic data [13-15], and it might be possible that this method would allow for some kind of correction to take place where a large solid volume, which is easily identifiable, shifts within the stack of tomographic images. Alternatively, in a solidified matrix where the sample has reached significant dimensional stability, some kind of bulk correction may also be attempted. While a region may appear similar by eye, this is not necessarily the case below the isolated surface that can be viewed in a given tomographic slice, which may yield a false positive result where regression coefficients are calculated as a function of the entire depth.

Digital image cross correlation, however, considers only an isolated region of interest (ROI) in a two-dimensional image slice, and so neglects all time-dependent variation in the depth both above and below the ROI. In the analysis of tomographic data this method has previously been used to assess displacement fields in non-homogeneous samples [16] which respond to loading inhomogeneously through their cross section. The calculation of an entire displacement field seems to introduce excessive computational demands, however, when attempting to isolate only individual groups of particles for which in-plane rotation of the particles is not expected to be significant.

After initially discovering the challenge present in fully analysing these data it was quickly realised that template matching by fast normalised cross correlation [17] could be an effective method by a correction may be successfully carried out, while neglecting the geometric changes below the cross section of the reacting particle itself. By the fast normalised cross correlation method, a two-dimensional ROI (a template image) is slid across a two dimensional target slice, and a matrix correlation coefficient R for each position in the x, y surface computed. In the typical application of the algorithm, the maximum value within the resulting two dimensional array is determined, which yields the location at which the best match is located on the x, y surface. In a tomographic stack consecutive slices are produced through the entire depth of the volume within the field of view of the instrument, and so a slight extension to the traditional approach was required for this work.

Taken as a starting point for this study, digital image cross correlation methods have been successfully and extensively implemented and documented in a number of programming languages. In the Python language, scikit-image [18] allows for rapid implementation of the method in a semantic high-level programming language. Statically typed compiled languages such as C++ may allow for a higher execution speed, and in these cases normalised cross may be executed using, for example, the OpenCV library[19]. For the most rapid testing of the discussed method we opted here to develop the algorithm entirely using the scikit-image toolkit [18] in the Python language. Code for the entire procedure is provided as Supplementary Information.

Imaging the Cementitious Suspension

The cementitious precursors selected were a Hanson Ribblesdale Works CEM I 52.5N ordinary Portland cement (PC) and a Hanson REGEN blast furnace slag (BFS), which were blended in ratios of 100% PC and 25% PC/75% BFS. No water reducing admixtures or viscosity modifying agents were used. A water/solids mass ratio of 0.47 was selected to allow straightforward compaction into a 3.0 mm diameter borosilicate glass capillary without causing fracture of the 10 µm-thick wall. This value was found to be the lowest reasonable water/solids ratio at which the capillary could be loaded, and remains within the typical limits provided by BS 8500 for the water/cement ratio of conventional concretes [20]. Potable water was used to hydrate the cements. The coarsest fraction of the BFS (contributed by the Calumite in the blended BFS material) was removed from the powder blend prior to mixing with water, using a 500 µm sieve, to allow placement of the material without restriction at the entry. The cement mix was compacted by briefly applying an oscillating head to the side of the capillary, although the ability of the cement pastes to retain air, and the narrow diameter of the capillary, complicated the compaction process significantly, and therefore regions of entrapped air remained within the matrix. These moved toward the top of the capillary during analysis of the fluid pastes, which caused the suspension to displace the rising volume and fall vertically through the stack. This is the most notable effect causing the movement of particles within the tomographic stack as successive images were collected, and which was corrected for in this paper.

The demonstration of this method is based on data collected at the 2-BM microtomography beamline at the Advanced Photon Source of Argonne National Laboratory [21], and analyses tomographic images acquired from tomographic data collected in-situ of reacting Portland cement-based materials. Here, we present a working correction for any geometric deviation in all materials studied. The application of this methodology to additional paste formulations is described in detail elsewhere [22], as the focus of this paper is the presentation and demonstration of the methodology.

The hydrating materials were rapidly scanned during the first minutes of the reaction before geometric stability was apparent, and during which sedimentation of the pastes was most evident. Acquisitions were scheduled at a time interval of approximately 10 seconds; for each, 600 radiographic projections were acquired by a pco.edge Dimax sCMOS high speed camera at 2000 fps, where this high frame rate was used to minimise the movement within the sample during each acquisition. Data were periodically discharged to magnetic storage for reconstruction off-line. The configuration provided a voxel size of 2.0 µm. Reconstruction was carried out using the TomoPy toolkit [23] developed in-house at the Advanced Photon Source synchrotron. Acquisitions were corrected for dark current and open beam artefacts, and were de-striped using the Fourier wavelet method[24]. Reconstruction was subsequently carried out using the Fourier grid reconstruction algorithm [25], for rapid implementation and code debugging.

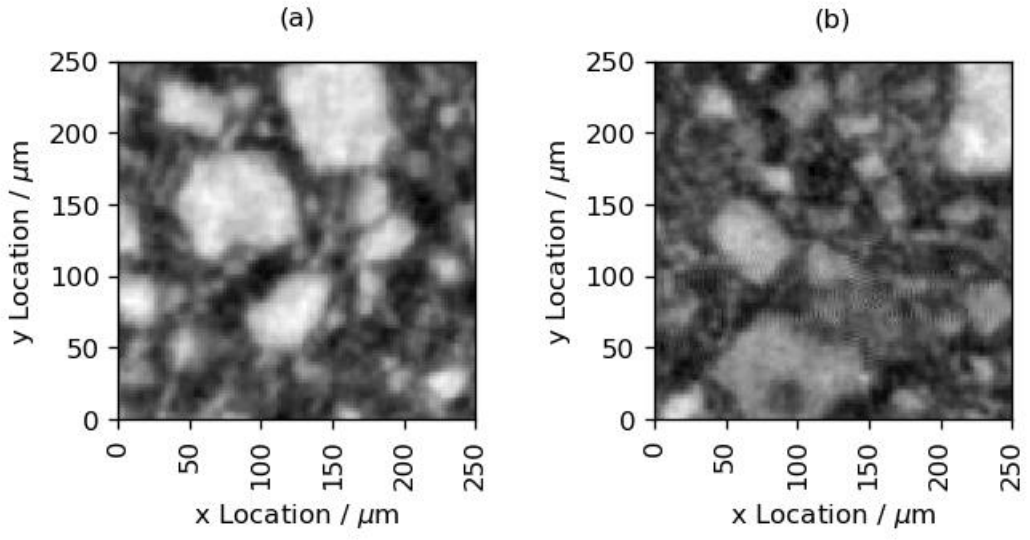

Figure 1 - Selected regions of interest from the 100% PC (a) and the 25% PC/75% BFS binders (b), 5 minutes after initiation of hydration.

Once reconstruction was completed, a single region of interest of 250 µm x 250 µm was manually selected from the first scan of each sample, as shown in Figure 2. Figure 2(a) shows the plain Portland cement material, while 2(b)

shows the cement with 75% BFS. Regions were isolated in the first reconstructed dataset, selected to be no less than 5 µm from any entrapped air or the capillary wall, to prevent a region being selected where the presence of a surface results in excessive rotation of particles within the volume of interest. This was verified in the x, y, and z axes after selection of the volume.

The procedure used is shown in Figure 2. Following manual selection of the target region of interest, a correlation coefficient was determined in every x, y location in every slice (z) in every stack (t), in the manner described above. The original slice was used as the template, and each interrogated slice as the searched plane, within the depth of the reconstructed volume. Once calculated, the maximum for each slice was subsequently written to a three dimensional array which contained the location in the x, y plane at which the region was located, and the R score at said maximum. The argument to the maximum of the R score contained within this array was then determined. This revealed the z location of the best match. The stored locations at this maximum score provide the position of the region of interest in all axes.

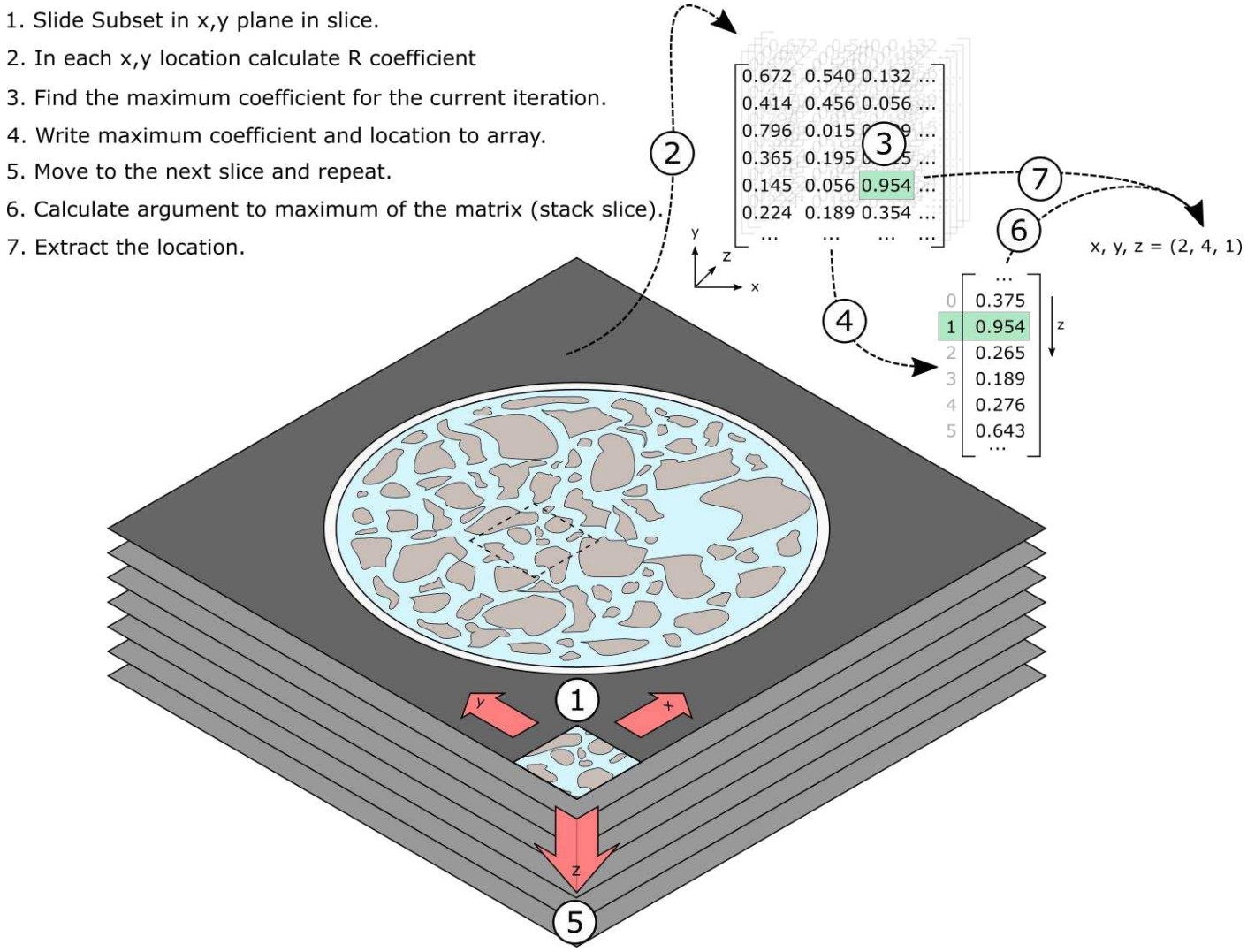

Figure 2 - The template matching procedure described in this paper.

In order to debug code and for a rapid verification of the method, scanning for the selected region of interest was back-applied to the first stack; this should provide a score of precisely unity at the location from which the subset was originally segmented, as in this position the template image and slice data must be identical. As expected, this was indeed found to be the case for the implementation described here.

Each stack was entirely analysed in approximately 3.5 minutes on a desktop workstation (Intel Core i7 4770K, 32 GB RAM, GNU/Linux 5.1.9).

Results and Discussion

Results from the slag-containing cementitious blend (25% PC/75% BFS) are shown in Figure 3. The regions shown are cropped directly from the stack, with corrected regions in (a) and uncorrected regions in (b). The images shown are 250 µm by 250 µm in cross sectional dimension. Part (c) shows the regression coefficient in each resolved location, and (d) the absolute degree of movement of the region of interest within the overall sample.

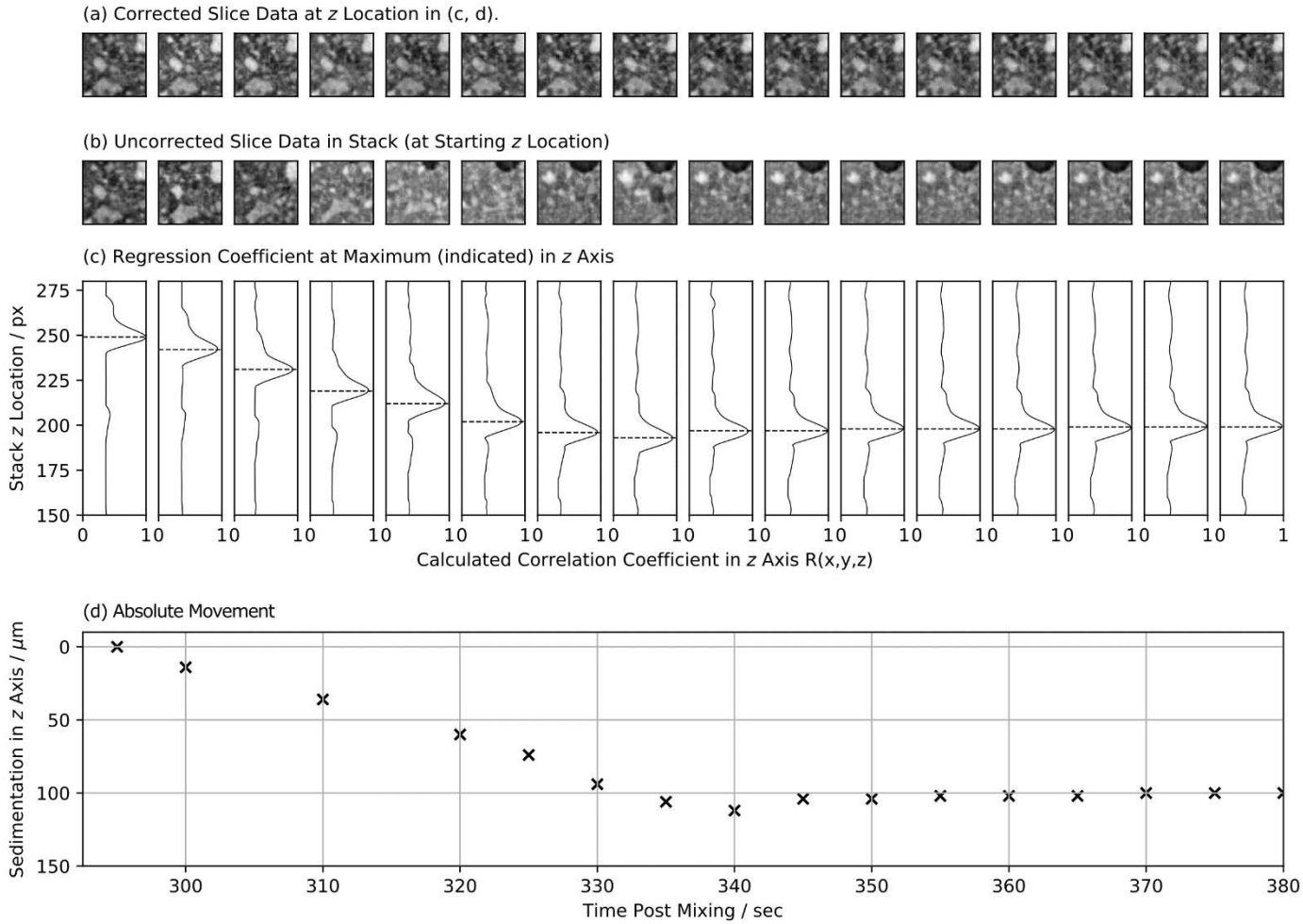

Figure 3 - Results from the BFS-containing cement blend.

The suspended particles in the region of interest have been located in the longer-time scans approximately 100 µm vertically below the position at which they were originally located. The correlation coefficients are high, and Figure 3a shows a clear similarity between the identified region at all time intervals, indicating that differential sedimentation of particles is not problematic for the application of this technique, within the particle size range present in the cementitious blend and observable by tomography here. The movement in this case occurs during the first seconds of the experimental time-frame, and the material reaches stability within the glass capillary as air rises and solid material falls. From the data here the same volume has been segmented from the stack; the application of the method has been successful.

Having established that this technique is reliable when analysing a relatively stable material, the next logical step is to carry out the analysis on a material which shows a more considerable movement of the region of interest within the stack. Figure 4 shows the application of the correction to the case of sedimentation of the pure PC suspension, which exhibits more significant particle movement through the volume of the sample, as the paste is less viscous and particle sedimentation is significant.

Across the duration of the reaction, no significant rotational variation is observed as the region of interest drops through the capillary. This allows, in the case of this material, for straightforward cropping of the desired particle volume by array slicing. Again, there is little differential movement of particles of different sizes within the timeframe studied.

The application of the method appears to have yielded a correct identification of the region of interest in both of these key test cases. All peak correlation coefficients extracted remain above 0.92. The method has revealed what appears to be a statistically probable match in all cases.

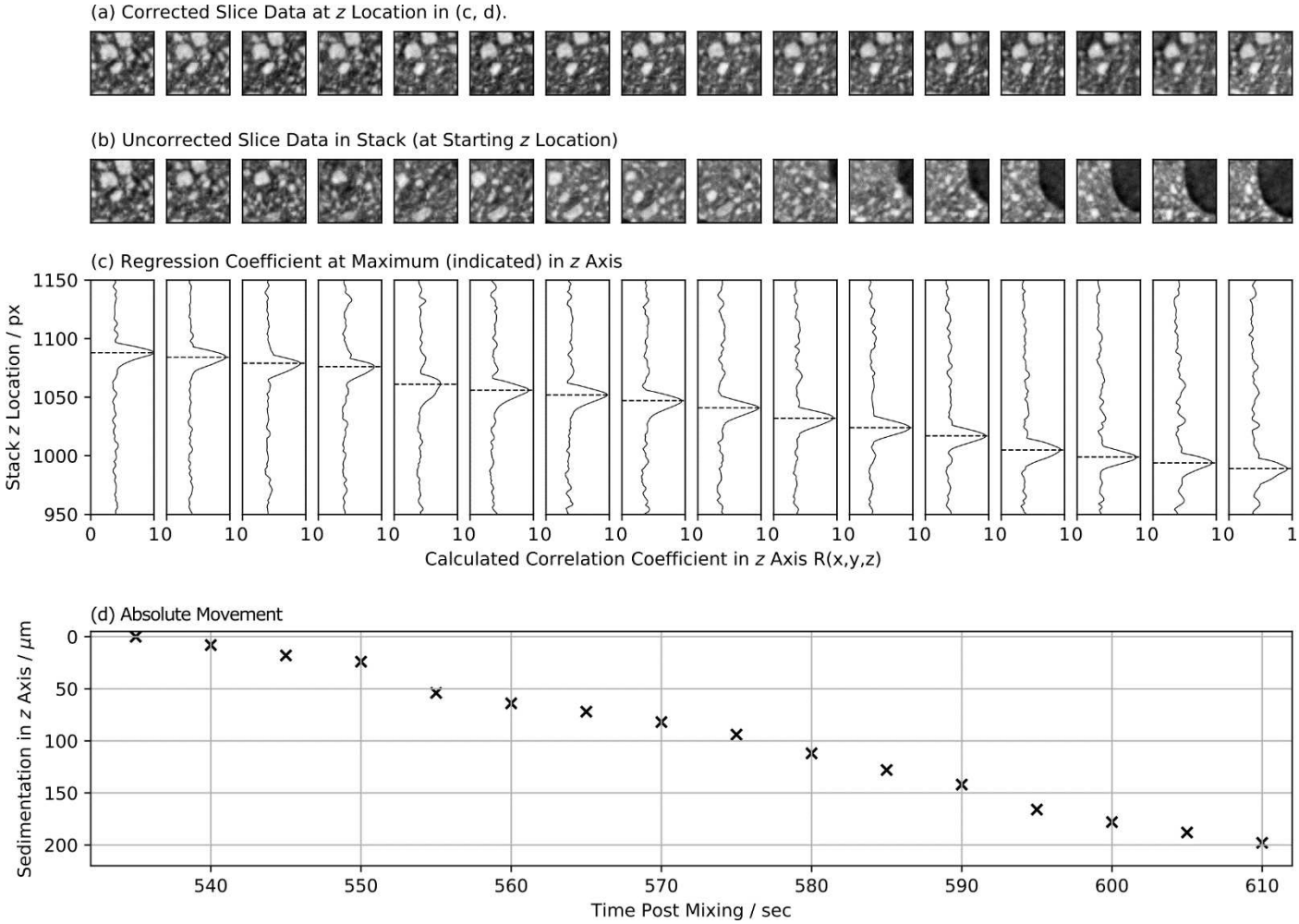

Figure 4- Results from the pure Portland cement sample.

Our method significantly reduces the human input requirement of high volume data segmentation, and additionally eliminates human bias. Without the assistance of a validated algorithm, this process would remain at best challenging, or more likely impossible.

Further to this, we predict that some modification to this analysis will result in a decrease in execution time, if correctly carried out. Knowing the density of the constituents of the suspension in the capillary, it may be possible to predict the direction of movement of the sample, and subsequently neglect regions into which movement of the sample is unlikely or not possible. Isolation of the movement of particles of specific size fractions as a function of time in dynamically moving suspensions may also offer the opportunity to assess the characteristics (e.g. viscosity) of the interstitial fluid via Stokes' Law or other comparable relationships, where this information is otherwise difficult to access.

Understanding some kind of mechanism by which the maximisation of the coefficient may be reliably characterised, will enable material below the isolated volume of interest to be neglected in cases where a good match has been previously identified, to further accelerate the calculation. This approach, and/or repeated calculations with re-

windowing of the region of interest in the x and/or y dimensions, may also reduce the likelihood of hitting a local maximum in the correlation coefficient that would give a spurious identification of the particle(s) of interest. However, such instances were not identified in the application of this method to the case studies presented in this paper, nor in any of the broader study of the authors where the methodology is ongoingly being applied to different cementitious pastes.

Conclusions

Our results demonstrate the full implementation and verification of an automated volume tracking methodology for analysing in-situ computed tomography data collected in suspensions containing highly reactive particles, in this case Portland cement. The method could similarly be applied to other colloidal suspensions with similar characteristics, if imaged in a time-resolved manner. This analysis has allowed us to track a unique region of interest across the first minutes of the experiment, providing us with access to data which would otherwise be impossible to isolate as particle locations move within a stack of tomographic slices displaying a complex microstructure. Without such a correction for the sedimentation and/or settlement of the material, tomographic scans collected prior to the material reaching stability would be either discarded, or it would remain impossible to isolate a precise particle group across the entire duration.

Acknowledgements

This work was carried out as a part of APS beamtime proposal GUP 40230 on the 2-BM-A,B endstation. This research used resources of the Advanced Photon Source, a U.S. Department of Energy (DOE) Office of Science User Facility operated for the DOE Office of Science by Argonne National Laboratory under Contract No. DE-AC02-06CH11357. This project is part funded by the Nuclear Decommissioning Authority (NDA) of the United Kingdom, and the Engineering and Physical Sciences Research Council (EPSRC), through a CASE Award studentship. Participation of S.A. Bernal in this study was sponsored by EPSRC through EC fellowship EP/R001642/1.

Conflicts of Interest

There are no conflicts of interest to declare.

References

1. D.P. Bentz, N.S. Martys, P. Stutzman, M.S. Levenson, E.J. Garboczi, J. Dunsmuir, and L.M. Schwartz, *X-ray microtomography of an ASTM C109 mortar exposed to sulfate attack.* Materials Research Society Symposium Proceedings, 1994. **370**: p. 77-82.
2. E. Gallucci, K. Scrivener, A. Groso, M. Stampanoni, and G. Margaritondo, *3D experimental investigation of the microstructure of cement pastes using synchrotron X-ray microtomography (μCT).* Cement and Concrete Research, 2007. **37**(3): p. 360-368.
3. M. Moradian, Q. Hu, M. Aboustait, M.T. Ley, J.C. Hanan, X. Xiao, V. Rose, R. Winarski, and G.W. Scherer, *Multi-scale observations of structure and chemical composition changes of portland cement systems during hydration.* Construction and Building Materials, 2019. **212**: p. 486-499.
4. Y. Wang, F. De Carlo, D.C. Mancini, I. McNulty, B. Tieman, J. Bresnahan, I. Foster, J. Insley, P. Lane, G. von Laszewski, C. Kesselman, M.-H. Su, and M. Thiebaux, *A high-throughput x-ray microtomography system at the Advanced Photon Source.* Review of Scientific Instruments, 2001. **72**(4): p. 2062-2068.
5. F. Fusseis, X. Xiao, C. Schrank, and F. De Carlo, *A brief guide to synchrotron radiation-based microtomography in (structural) geology and rock mechanics.* Journal of Structural Geology, 2014. **65**: p. 1-16.
6. A. du Plessis and W.P. Boshoff, *A review of X-ray computed tomography of concrete and asphalt construction materials.* Construction and Building Materials, 2019. **199**: p. 637-651.
7. J.L. Provis, R.J. Myers, C.E. White, V. Rose, and J.S.J. van Deventer, *X-ray microtomography shows pore structure and tortuosity in alkali-activated binders.* Cement and Concrete Research, 2012. **42**(6): p. 855-864.
8. E.J. Garboczi and J.W. Bullard, *Shape analysis of a reference cement.* Cement and Concrete Research, 2004. **34**(10): p. 1933-1937.

9. T. Lowe, R.J. Garwood, T.J. Simonsen, R.S. Bradley, and P.J. Withers, *Metamorphosis revealed: time-lapse three-dimensional imaging inside a living chrysalis.* Journal of The Royal Society Interface, 2013. **10**(84): #20130304.
10. S.M. Walker, D.A. Schwyn, R. Mokso, M. Wicklein, T. Müller, M. Doube, M. Stampanoni, H.G. Krapp, and G.K. Taylor, *In vivo time-resolved microtomography reveals the mechanics of the blowfly flight motor.* PLOS Biology, 2014. **12**(3): e1001823.
11. M. Saric-Coric, K.H. Khayat, and A. Tagnit-Hamou, *Performance characteristics of cement grouts made with various combinations of high-range water reducer and cellulose-based viscosity modifier.* Cement and Concrete Research, 2003. **33**(12): p. 1999-2008.
12. C. Jolicoeur and M.-A. Simard, *Chemical admixture-cement interactions: Phenomenology and physico-chemical concepts.* Cement and Concrete Composites, 1998. **20**(2-3): p. 87-101.
13. A. Germaneau, P. Doumalin, and J.-C. Dupré, *Comparison between X-ray micro-computed tomography and optical scanning tomography for full 3D strain measurement by digital volume correlation.* NDT & E International, 2008. **41**(6): p. 407-415.
14. F. Forsberg, M. Sjödahl, R. Mooser, E. Hack, and P. Wyss, *Full three-dimensional strain measurements on wood exposed to three-point bending: analysis by use of digital volume correlation applied to synchrotron radiation micro-computed tomography image data.* Strain: An International Journal for Experimental Mechanics, 2010. **46**(1): p. 47-60.
15. B.K. Bay, T.S. Smith, D.P. Fyhrie, and M. Saad, *Digital volume correlation: Three-dimensional strain mapping using X-ray tomography.* Experimental Mechanics, 1999. **39**(3): p. 217-226.
16. E. Tudisco, E. Andò, R. Cailletaud, and S.A. Hall, *TomoWarp2: A local digital volume correlation code.* SoftwareX, 2017. **6**: p. 267-270.
17. J.-C. Yoo and T.H. Han, *Fast normalized cross-correlation.* Circuits, Systems and Signal Processing, 2009. **28**(6): p. 819-843.
18. S. Van der Walt, J.L. Schönberger, J. Nunez-Iglesias, F. Boulogne, J.D. Warner, N. Yager, E. Gouillart, and T.J.P. Yu, *scikit-image: image processing in Python.* PeerJ, 2014. **2**: e453.
19. I. Culjak, D. Abram, T. Pribanic, H. Dzapo, and M. Cifrek. *A brief introduction to OpenCV*. in *2012 Proceedings of the 35th International Convention MIPRO*. Opatija, 2012, pp. 1725-1730.
20. *BS 8500: Complementary British Standard to BS EN 206*. 2015, BSI (British Standards Institution): London, UK.
21. X. Xiao, F. Fusseis, and F.D. Carlo. *X-ray fast tomography and its applications in dynamical phenomena studies in geosciences at Advanced Photon Source*. SPIE Optical Engineering + Applications, 2012. **8506**: #85060K.
22. J.E. Vigor, *Photons and subatomic particles. what can these tell us about cements, moisture, and nuclear waste?*, Ph.D. thesis, Department of Materials Science and Engineering, The University of Sheffield, 2019.
23. D. Gursoy, F. De Carlo, X. Xiao, and C. Jacobsen, *TomoPy: a framework for the analysis of synchrotron tomographic data.* Journal of Synchrotron Radiation, 2014. **21**(5): p. 1188-1193.
24. B. Münch, P. Trtik, F. Marone, and M. Stampanoni, *Stripe and ring artifact removal with combined wavelet — Fourier filtering.* Optics Express, 2009. **17**(10): p. 8567-8591.
25. M.L. Rivers, *tomoRecon: High-speed tomography reconstruction on workstations using multi-threading*. SPIE Optical Engineering + Applications, 2012. **8506**: #85060K